Supporting Information

A pinecone-inspired nanostructure design for long-cycle and high performance Si anode

Yinghui Xue, Jingwen Deng, Cheng Wang, Rafael G. Mendes, Linfeng Chen, Yao Xiao, Qin Zhang, Tao Zhang, Xuebo Hu, Xianglong Li, Mark H. Rümmeli, Lei Fu*

Figure S1. XPS of SiO_2@GF and encapsulated Si. (a), (b) Si 2p states and O 1s states of SiO_2-GF. (c) Si 2p states of encapsulated Si, the transformation from (a) to (c) shows clearly the conversion of Si–O–Si bond to Si–Si bond through magnesium thermal reduction. (d) XPS survey spectrum of SiO_2-GF and uE-Si, demonstrating the successful reduction of silica to silicon during the magnesium thermal reduction.

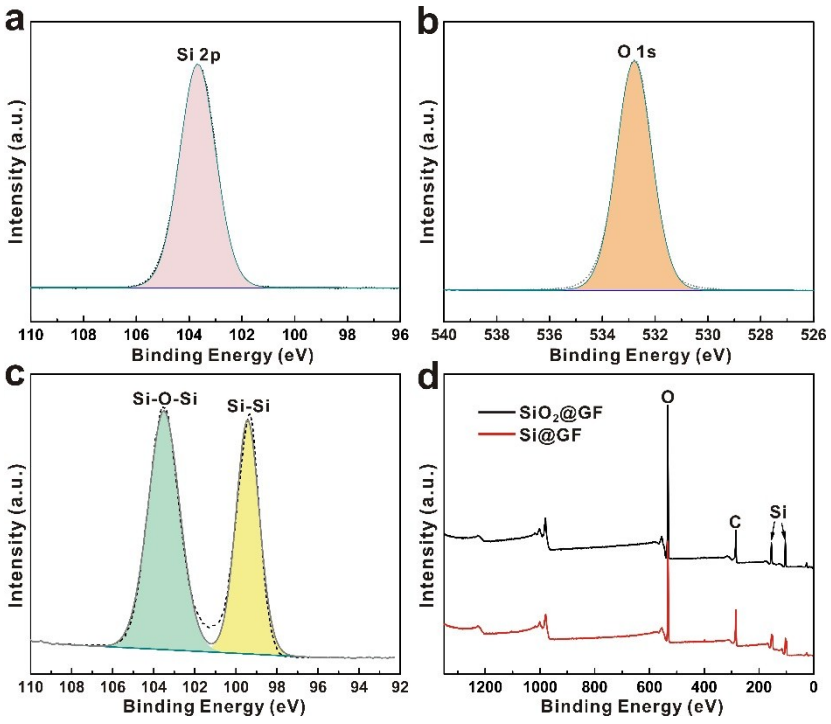

Figure S2. SEM and TEM images of GF, SiO_2-GF and uE-Si (a) SEM image of GF, a smooth surface with some wrinkles. (b) SEM image of SiO_2-GF, close contact between SiO_2 and GF is achieved by SCF method. (c) TEM image of SiO_2-GF, graphene is coated with a thick layer of amorphous SiO_2, as confirmed by the diffraction inset. (d) HRTEM image of SiO_2-GF, confirms the presence of amorphous SiO_2 and graphene. (e) TEM image of uE-Si, as a supporter, GF is loaded with Si nanoparticles. (f) HRTEM image of uE-Si confirms the presence of crystalline Si (111), as well as an amorphous SiO_2 layer on the surface of Si.

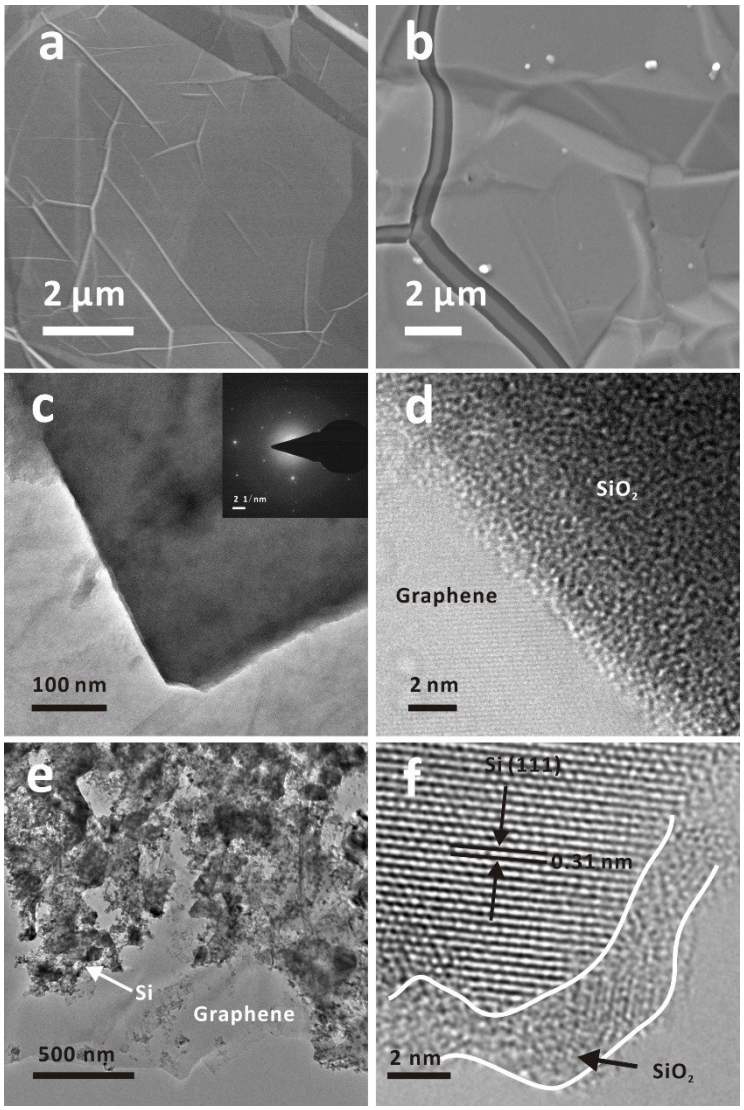

Figure S3. SEM and Characterizations of uE-Si and GE-Si after cycling and statistical analysis of the diameters of GE-Si and uE-Si before and after cycling. (a) SEM image of uE-Si after cycling at low magnification shows severe aggregation. (b) an enlarged image of (a) shows expansion and various particle sizes. (d) SEM image of GE-Si after cycling at low magnification reveals a uniform particle size. (e) enlarged image of (d) shows the porous structure remains, indicating a reversible expansion/contraction process. (c) Particle diameters distribution of GE-Si and uE-Si before cycling. (f) Particle diameters distribution of GE-Si and uE-Si after cycling.

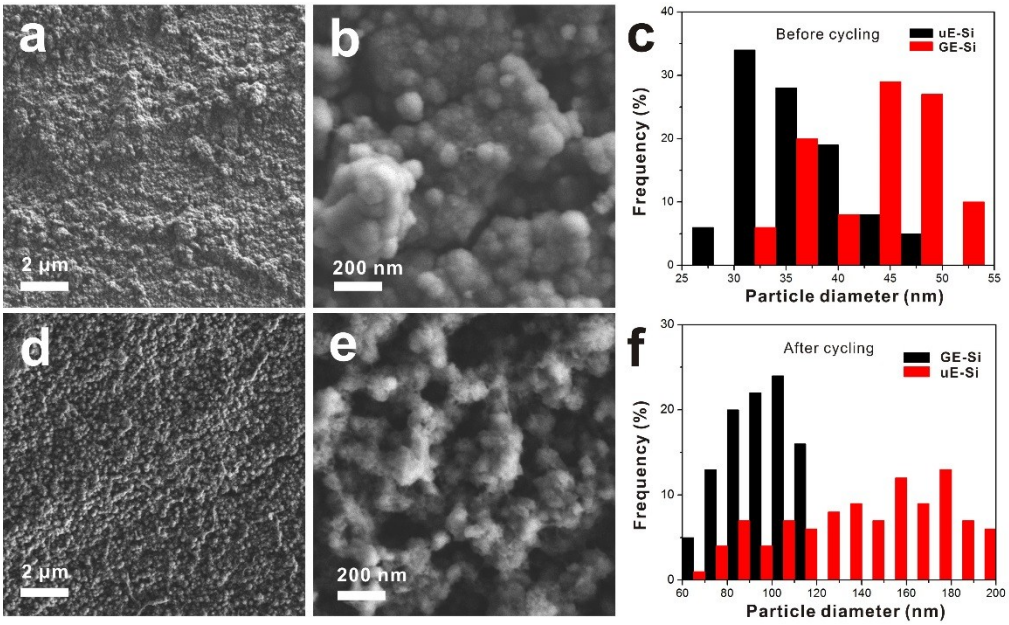

Figure S4. Raman spectra of (a) GF and (b) GE-Si composite. In **Figure S**4a, the Raman intensity of the G band is higher than the 2D band, which is consistent with the multilayer property of the graphene foam. The low intensity of the D bands centred at 1350 cm^{-1} implies a high quality for the GF. In **Figure S**4b, the peak at ~520 cm^{-1} corresponds to the characteristic band of single crystalline silicon. The relatively higher intensity of the D band than that of the G band mainly results from the partially-disordered structure of the overlapped graphene sheets. The absence of GF may be attributed to the covering of a thick Si layer.

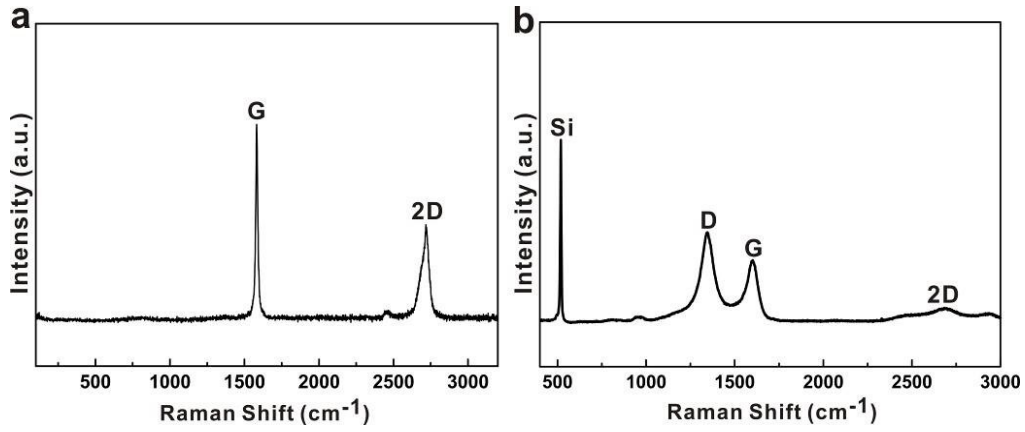

Figure S5. Thermal gravimetric analysis (TGA) of GE-Si composite. The mass loss at about 700 ^{o}C is caused by the decomposition of GF and graphene in GE-Si. The mass increased after 900 ^{o}C because of the oxidation of Si. The result indicates the GE-Si composite is consisted of 52.9% Si and 47.1% graphene.

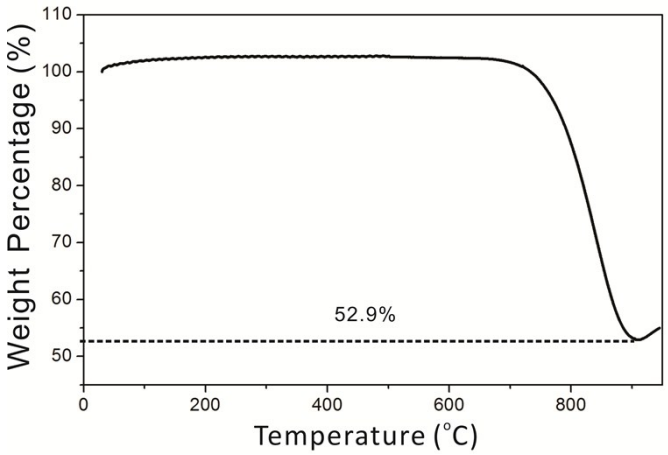

Figure S6. A comparison of electrochemical performance of pinecone-like GE-Si electrode with recent studies on Si-based anodes. (a) Comparison of capacity in different cycle numbers. (b) Comparison of capacity in different current density.[1–10]

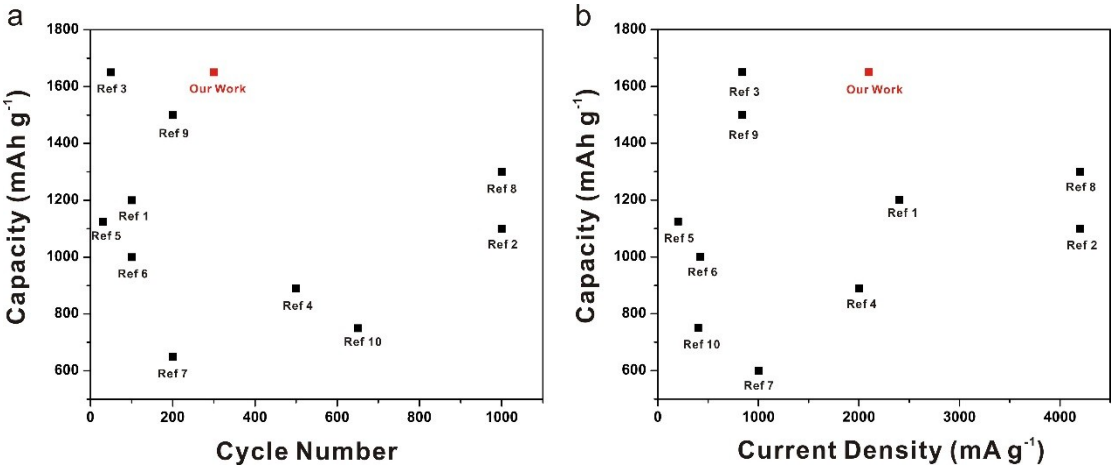

Reference

1. J. Chang, X. Huang, G. Zhou, S. Cui, P. B. Hallac, J. Jiang, P. T. Hurley, J. Chen, *Adv. Mater.* 2014, **26**, 758.
2. B. Wang, X. Li, X. Zhang, B. Luo, Y. Zhang, L. Zhi, *Adv. Mater.* 2013, **25**, 3560.
3. B. Wang, X. Li, X. Zhang, B. Luo, M. Jin, M. Liang, S. A. Dayeh, S. T. Picraux, L. Zhi, *ACS Nano* 2013, **7**, 1437.
4. B. Wang, X. Li, B. Luo, L. Hao, M. Zhou, X. Zhang, Z. Fan, L. Zhi, *Adv. Mater.* 2015, **27**, 1526.
5. X. Meng, D. Deng, *ACS Appl. Mater. Interfaces* 2015, **7**, 6867.
6. B. Wang, X. Li, B. Luo, X. Zhang, Y. Shang, A. Cao, L. Zhi, *ACS Appl. Mater. Interfaces* 2013, **5**, 6467.
7. F. Zhang, X. Yang, Y. Xie, N. Yi, Y. Huang, Y. Chen, *Carbon* 2015, **82**, 161.
8. N. Liu, H. Wu, M. T. McDowell, Y. Yao, C. Wang, Y. Cui, *Nano Lett.* 2012, **12**, 3315.
9. B. Wang, X. Li, T. Qiu, B. Luo, J. Ning, J. Li, X. Zhang, M. Liang, L. Zhi, *Nano Lett.* 2013, **13**, 5578.
10. Z. Favors, H. H. Bay, Z. Mutlu, K. Ahmed, R. Lonescu, R. Ye, M. Ozkan, C. S. Ozkan, *Sci. Rep.* 2015, **5**, 8246.